International Journal of Peptide Research and Therapeutics (2025) 31:3
https://doi.org/10.1007/s10989-024-10662-2

Diastereomers of the Anticancer Peptide CIGB-300 with Altered β-Turn Structures

Celia G. Moya[1,2] · Rafael Rodriguez[2] · Carlos S. Perez[2] · Hilda Garay[3] · Julian Wiesent[1] · Stefan Gröger[1] · Yordanka Masforrol[3] · Yasser Perera[3] · Silvio E. Perea[3] · Jochen Balbach[1]

Accepted: 17 October 2024 / Published online: 5 November 2024

Abstract

Purpose The next-generation anti-tumor drug peptide CIGB-300, developed by the Center for Genetic Engineering and Biotechnology (CIGB), targets casein kinase 2 (CK2) and its substrates, implicating significant therapeutic potential in cancer treatment. A key focus of this study was to compare CIGB-300 and a primary synthetic byproduct, CIGB-300iso, which shares the amino acid sequence with CIGB-300 but was proposed to differ due to racemization.

Methods This study explores the synthesis, characterization, and structural elucidation of CIGB-300 and its isomer CIGB-300iso by a comprehensive NMR analysis of seven synthesized diastereomers including amino acid residues C15, H21, and C25.

Results This study revealed that CIGB-300iso contains one D enantiomer at position H21. The structures of both isoforms derived from NMR constraints disclosed that the L and D enantiomers have an altered peptide supersecondary structure, with a β-turn type IV_3 found in CIGB-300 and a type I β-turn in CIGB-300iso.

Conclusion The configuration of H21 significantly impacts the peptide's conformations, sidechain orientations and, potentially, its biological activity. These findings highlight the importance of enantiomerically pure peptides for the design and synthesis of drug peptides.

Keywords CIGB300 · Peptide · NMR · Histidine racemization · Peptide enantiomers · Cyclic peptide

Introduction

CIGB-300, a peptide drug developed by the Center for Genetic Engineering and Biotechnology (CIGB) in Havana, Cuba, is undergoing clinical trials as a next-generation anti-tumor medication for cervix cancer (Perera et al. 2012). This particular peptide interacts with casein kinase 2 (CK2) and its substrates (Perera et al. 2020; Pérez et al. 2023), both of which play crucial roles in numerous biological processes (Trembley et al. 2009; Ahmed et al. 2015; Roffey and Litchfield 2021). CK2 is a very well-conserved serine/threonine kinase involved in the phosphorylation of many substrates, which displays a very conserved acidic phosphorylation domain (Niefind et al. 2001). CK2 is essential for different cell functions like gene expression, cell growth, cell survival, chromatin remodeling, and protection of cells against apoptosis (Roffey and Litchfield 2021). For this reason, searching for new CK2 inhibitors might become valuable for cancer therapy.

The CIGB-300 peptide consists of 25 amino acids (Fig. 1). The sequence from 1 to 13 corresponds to the TAT cell-penetrating peptide (G^{48}RKKRRQRRRPPQ^{60}), while the sequence from 15 to 25 (C^{15}WMSPRHLGTC^{25}) corresponds to a cyclic part resulting from the disulfide bond of the two terminal cysteines. These two sections are connected by a beta-alanine spacer (-βA-) (Garay et al. 2018).

CIGB-300 is synthesized via solid-phase peptide synthesis (SPPS) utilizing the conventional Fmoc/tert-Butyl chemistry (Behrendt et al. 2016). Following cleavage, the crude material is cyclized through the spontaneous air oxidation of the C15 and C25 thiol groups in a diluted solution under

✉ Jochen Balbach
jochen.balbach@physik.uni-halle.de

1 Martin Luther University Halle-Wittenberg, Halle-Saale, Germany

2 University of Havana, Havana, Cuba

3 Center for Genetic Engineering and Biotechnology, Havana, Cuba

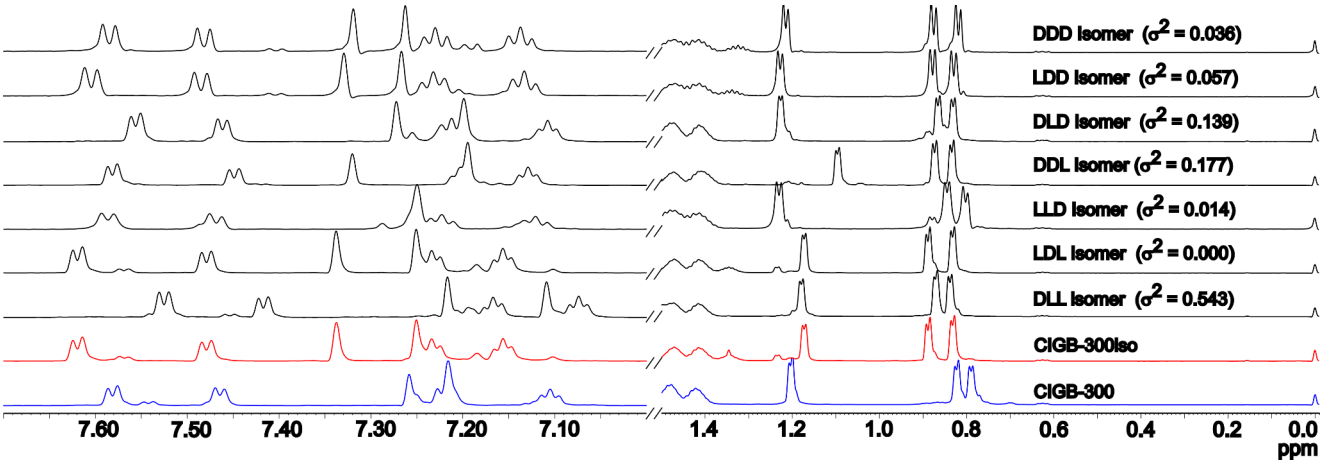

Fig. 1 Comparison of the 1D ^{1}H NMR spectra of CIGB-300 (blue), and CIGB-300iso (red) with the spectra of synthesized diastereomers (black): DLL, LDL, LLD, DDL, DLD, LDD, DDD, where each letter corresponds to the L or D configuration of C15, H21, and C25 respectively. The variance of the corresponding synthesized isomers in parenthesis is reported in respect to the CIGB-300iso spectrum

alkaline conditions (Chiari et al. 1990), yielding a monomeric cyclic peptide through an intramolecular disulfide bond. The cyclic peptide is subsequently purified through reverse-phase (RP) HPLC, ensuring a purity level of ≥ 97% that adheres to the batch release criteria endorsed for this drug substance by the Quality Control Department of the CIGB.

A study conducted by Garay et al. utilized mass spectrometry to identify and analyze the primary byproducts that emerge from the synthesis of CIGB-300 according to the ICHQ3A(R2) guidelines (Garay et al. 2018). This analysis revealed that one major byproduct (in this report called CIGB-300iso) had the same amino acid sequence as CIGB-300, but potentially, a racemization of cysteine and/or histidine residues occurs during the coupling process (Garay et al. 2018). It is very well reported that peptides containing these two amino acids can racemized by base-catalyzed coupling to the resin (Kovacs et al. 1985; Han et al. 1997).

A correct activation strategy of the carboxylate is necessary to avoid two common undesired reactions in SPPS: 1 - the racemization that affects Cα by extensive pre-activation due to intramolecular abstraction of Hα by Nπ from the imidazolyl side chain with the reprotonation of the resulting carbanion; 2 - the Nα-endcapping with DIC by the in situ activation. The success of the synthesis depends on the balance of these reactions (Yang et al. 2022). A standard amount of the CIGB-300iso was obtained with a long pre-activation time of ten minutes at 25 ºC for each Fmoc-L-amino acid and 60 min for the coupling reactions. However after purification by RP-HPLC, this impurity represented 0.13% of all peptide components as reported by (Garay et al. 2018). Characterizing and identifying this isomer peptide is of utmost importance, as it constitutes one of the main contaminants in the crude form of CIGB-300. Furthermore, it can be isolated in sufficient quantities after the HPLC purification, allowing detailed mass spectrometry and NMR characterization.

In the presented report, we show an extended NMR analysis of various diastereomers of CIGB300. Also, the CIGB-300iso byproduct contains a D-histidine at position 21 in the cyclic part of the peptide. For both enantiomers CIGB-300 and CIGB-300iso, we determined the NMR structure and found two different β-turn arrangements depending on the D or L configuration of H21. This might impair the inhibitory function of both isomers because of the altered orientation of several side chains.

Materials and methods

Peptide Synthesis and Purification

The CIGB-300 peptide and its variants were synthesized manually through solid-phase chemistry on Aminomethyl-ChemMatrix resin (Iris Biotech GmbH, 0.49mmol/g) by a stepwise solid-phase procedure using the Fmoc/tertButyl chemistry (Fields and Noble 1990). The Fmoc-L-amino acid was coupled by activation with Oxyma pure/N, N'-diisopropylcarbodiimide (Oxyma/DIC), in a four times molar excess in DMF (Subirós-Funosas et al. 2009). The Fmoc-D-amino acids were utilized for substituting Cys and/or His at positions 15, 21, and/or 25 within the peptide sequence (refer to Table 1). A two-fold excess of Oxyma/DIC and D-aminoacids and more time for the reaction were used for coupling the D-amino acids. The ninhydrin test confirmed the completion of peptide bond formation (Kaiser et al. 1970). The Fmoc group was removed with 20% piperidine/N-N-dimethylformamide. To remove side chain-protecting

Table 1 CIGB-300 peptide variants by D-amino acids substitution

Sequence	Code for L or D configuration of C15, H21, and C25
GRKKRRQRRRPPQ-βA-**C***WMSPRHLGTC	DLL
GRKKRRQRRRPPQ-βA-CWMSPR**H***LGTC	LDL
GRKKRRQRRRPPQ-βA-CWMSPRHLGT**C***	LLD
GRKKRRQRRRPPQ-βA-**C***WMSPR**H***LGTC	DDL
GRKKRRQRRRPPQ-βA-**C***WMSPRHLGT**C***	DLD
GRKKRRQRRRPPQ-βA-CWMSPR**H***LGT**C***	LDD
GRKKRRQRRRPPQ-βA-**C***WMSPR**H***LGT**C***	DDD

Sequences and synthesis codes with (L or D) configuration for C15, H21, and C25 in the sequences of the peptides. D-Cys and D-His are indicated in the sequence with bold letters and an asterisk

groups and to ensure their cleavage from the resin, the treatment with trifluoroacetic acid (TFA)/H_2O/EDT/TIS (94/2.5/2.5/1) was completed in 2 h; the crude peptide was precipitated with cold diethyl ether, dissolved in 40% acetonitrile/water, and later lyophilized. The reduced peptide was dissolved in an aqueous solution (pH 8.2) at 0.5 mg/mL and cyclized through spontaneous air oxidation (Pennington and Dunn 1994) by gently stirring for 6 h. The peptides were purified by RP-HPLC, lyophilized, and identified by electrospray ionization mass spectrometry (ESI-MS; MW 3057.62 ± 0.5 Da, monoisotopic molecular mass).

NMR Measurements

The NMR samples for chemical shift assignment were prepared through the dissolution of the lyophilized peptide in a mixture consisting of distilled water and 10% D_2O to achieve a final concentration of about 3mM. For simplification of the aromatic region in the spectra, the respective peptide isomers were dissolved in D_2O for 1D ^{1}H-NMR comparisons. In addition, 0.03% DSS was added to all samples for chemical shift referencing (Morash et al. 2018), and the pH was maintained between 3.2 and 3.5 or 7.2. The measurements were conducted using a Bruker US2 800 Avance III spectrometer operating at a proton frequency of 800.23 MHz with a TXO cryoprobe. The WATERGATE pulse sequence was employed to suppress the water signal (Piotto et al. 1992). The NMR signals were assigned following the methodology established by Wüthrich (Wüthrich 1990), which entailed analyzing standard homonuclear experiments such as TOCSY (with a mixing time of 75 ms at 298 K), NOESY (with mixing times of 200, 300, 500, and 750 ms at 298 K), and additional heteronuclear natural abundance ^{13}C-HSQC and ^{13}C-HSQC-TOCSY experiments. All the NMR spectra were meticulously analyzed, assigned, and integrated using the NMR-FAM-Sparky-v-1.470.8 software package (Lee et al. 2015). Temperature coefficients for H^N protons were derived by following the H^N spin system in the TOCSY experiments at various temperatures (75 ms mixing time at 288 K, 293 K, 298 K, and 303 K). A linear regression of $\Delta\delta$ ($\delta_{Ti}-\delta_{T288}$) versus T was applied to determine the temperature coefficient for the individual H^N protons (Cierpicki and Otlewski 2001)

Comparison of NMR Data

The comparison of chemical shifts between CIGB-300 and CIGB-300iso was evaluated by subtracting the corresponding chemical of CIGB-300iso from CIGB-300. To evaluate the degree of overlap in the 1D-^{1}H-NMR spectra, we employ algorithms for variance-like calculation. This process involved automatically assigning signals in each spectrum using the NMRglue Python library and summing the squares of the differences between signals with chemical shift values closest to one another (Helmus and Jaroniec 2013).

Structure Calculation

The molecular structure was determined using a Simulated Annealing protocol implemented in the Xplor-NIHv3.8 software (Schwieters et al. 2003, 2006, 2018). Initial structures were generated and refined using tailored scripts from the input examples in the Xplor-NIHv3.8 documentation to employ only distance and dihedral angle constraints. Script aneal.py generated the first 200 structures, the lowest energy structure was used as input structures for refine.py to perform the refinement. The implicit solvent minimization was carried out with the 20 best structures from refinement (10% of lower energy structures) with the wreine.py script. The NOE contact intensities from NOESY data at 200 mixing time were used as distance constraints. Cross peaks in the NOESY spectrum with mixing times longer than 300ms are not satisfied by the structure calculation program, which is most likely due to spin diffusion. The NOESY signals were integrated with NMR-FAM-Sparky-v-1.470.8 and classified into three groups: weak (3.5 to 5.0 Å), medium (2.8 to 3.5 Å), and strong (1.7 to 2.8 Å). As a result, 196 distance restraints were imposed for CIGB-300 and 203 restraints for CIGB-300iso. The dihedral angles were predicted with TALOS-N(Shen and Bax 2015) and TALOS+ (Shen et al. 2009) and all predictions classified as good were used as restraints. In total 26 dihedral restrictions were imposed for CIGB-300 and 32 for CIGB-300iso and the corresponding statistics of the NMR structure calculations are reported in Table S7.

Results and Discussion

The NMR assignment of both peptides was accomplished following the traditional methodology based on 2D $^{1}H^{1}H$ NOESY and TOCSY. Also, ^{13}C edited HSQC data at natural abundance were used to assign carbon resonances and to solve ambiguities in the ^{1}H spectra to derive 98% ^{1}H and 95% ^{13}C assignments for both isomers. The chemical shifts of CIGB-300 and CIGB-300iso (Table S1) were compared to identify possible differences in peptide conformations. Overall, these differences were found to be rather small. The N-terminal amino acid chain corresponding to the TAT region G1-Q13 does not show considerable variations because chemical shift differences were less than 0.1 ppm for protons and 0.3 ppm for carbons. In contrast, residues in the cyclic part of the peptides (C15 – C25) showed notable differences (Figure S3). Inspection of the backbone proton chemical shifts revealed the largest differences for the Hα protons of M17 and H21 and the H^{N} protons of S18 and R20. This was the first indication that structural variations between the two CIGB-300 and its isomer are located in the cyclic peptide region. Due to a specific amino acid's L to D configuration change, the side chain orientations undergo a more pronounced alteration. Consequently, we also examined the side chain protons resonances, where we found that only H21 demonstrated an average difference of 0.15ppm, while for the other amino acids, it consistently remained below 0.05ppm. The carbon chemical shift comparison for the side chains yielded small changes only for C15, M17, H21, L22, and C25. At least one minor conformation was identifiable in the NMR spectra of both CIGB-300 isomers by some very weak extra signals, especially in the cyclic part in the corresponding TOCSY and NOESY spectra. These additional cross-peaks were assigned (Table S2). Because of the presence of three prolines, P11, P12, and P19, in CIGB-300, we consider that the additional observed conformers could be due to cis-trans equilibria, but in none of the spectra, we found additional signals for prolines. We also calculated δ(Cβ) - δ(Cγ), confirming that all prolines of the major conformer of both CIGB-300 isomers are in the trans conformation.

It has been reported that cysteine and mostly histidine residues are prone to racemization during peptide synthesis (Kovacs et al. 1985; Han et al. 1997; Yang et al. 2022). Based on that fact and the results from the chemical shift differences between CIGB-300 and CIGB-300iso, seven diastereomers with all combinations of D and L residues at positions C15, H21, and C25 were synthesized. Figure 1 shows the 1D ^{1}H-NMR spectra of these seven isomers compared to CIGB-300 and CIGB-300iso. An eye inspection revealed that the L-C15/D-H21/L-C25 isomer corresponded best to the spectrum of CIGB-300iso. A quantification by calculating the variance of the entire 1D spectrum further corroborates that this isomer is the only one where all the sidechain signals and the extra signals corresponding to minor conformations match CIGB-300iso.

In the next step, we compared the 2D NOESY spectra of CIGB-300 and CIGB-300iso to find possible structural rearrangements due to D-His21. Despite minimal changes in the distances of protons in most residues, NOE contacts for H21 revealed notable differences (Fig. 2). The NOESY spectra of CIGB-300iso contained, for example, NOEs between the sidechains of H21 and L22, not present in the CIGB-300 (red cross peak assignment in the top NOESY section of Fig. 2). Meanwhile, the β-protons of H21 showed contacts to the amide proton of S18 in CIGB-300 (blue assignment in the second NOESY section from the top in Fig. 2) which are not present in CIGB-300iso. The same holds for one β-proton of S18, which shows only in CIGB-300iso a contact to the amide proton of H21 (red assignment in the second spectrum from the bottom in Fig. 2) but not in CIGB-300 (missing cross peak in the bottom spectrum in Fig. 2). Another important difference was found for the orientation of the W16 side chain, which showed contacts to the amide proton of M17 in CIGB-300, but to the α-proton of C15 in CIGB-300iso. This different orientation could explain why M17 shows the biggest difference in the Hα/Cα chemical shift analysis.

For a very detailed comparison of CIGB-300 and CIGB-300iso and to further study the influence of D- instead of L-His21, their three-dimensional structures based on the distance constraints derived from NOEs and dihedral angles were determined by simulated annealing with the Xplor program package. A superposition of the 20 structures of lowest energies for both peptides of the region corresponding to the linear part (residues Gly1 – βAla14) showed an extended but otherwise featureless conformation for both peptides and no restricted orientation towards the cyclic parts (Fig. S4). On the other hand, the superposition of the cyclic region showed a much more well-defined structure in both peptides (Fig. 3A and C). The cyclic part of the CIGB-300 revealed three loops (Fig. 3B), with the first loop formed by C15 to S18, the second loop by S18 to H21, and a slightly less defined third loop from L22 to C25. The three loops show distances between C_{α} of residue i and i + 3 shorter than 7Å, classifying them as β-turns (Lewis et al. 1973; Chou 2000). The first and third loops are open-turns (Chou 2000) with an average distance between the C_{α} carbons of C15 and S18 of 5.47 ± 0.56 Å (cyan in Fig. 3B) and L22 and C25 of 5.79 ± 0.91 Å (magenta in Fig. 3B). The second loop is stabilized by a hydrogen bond between the carbonyl group of S18 and the amide proton of H21 (black dotted line in Fig. 3B) leading to an average distance between C_{α} of the mentioned residues of 5.20 ± 0.27 Å. The H^{N} temperature

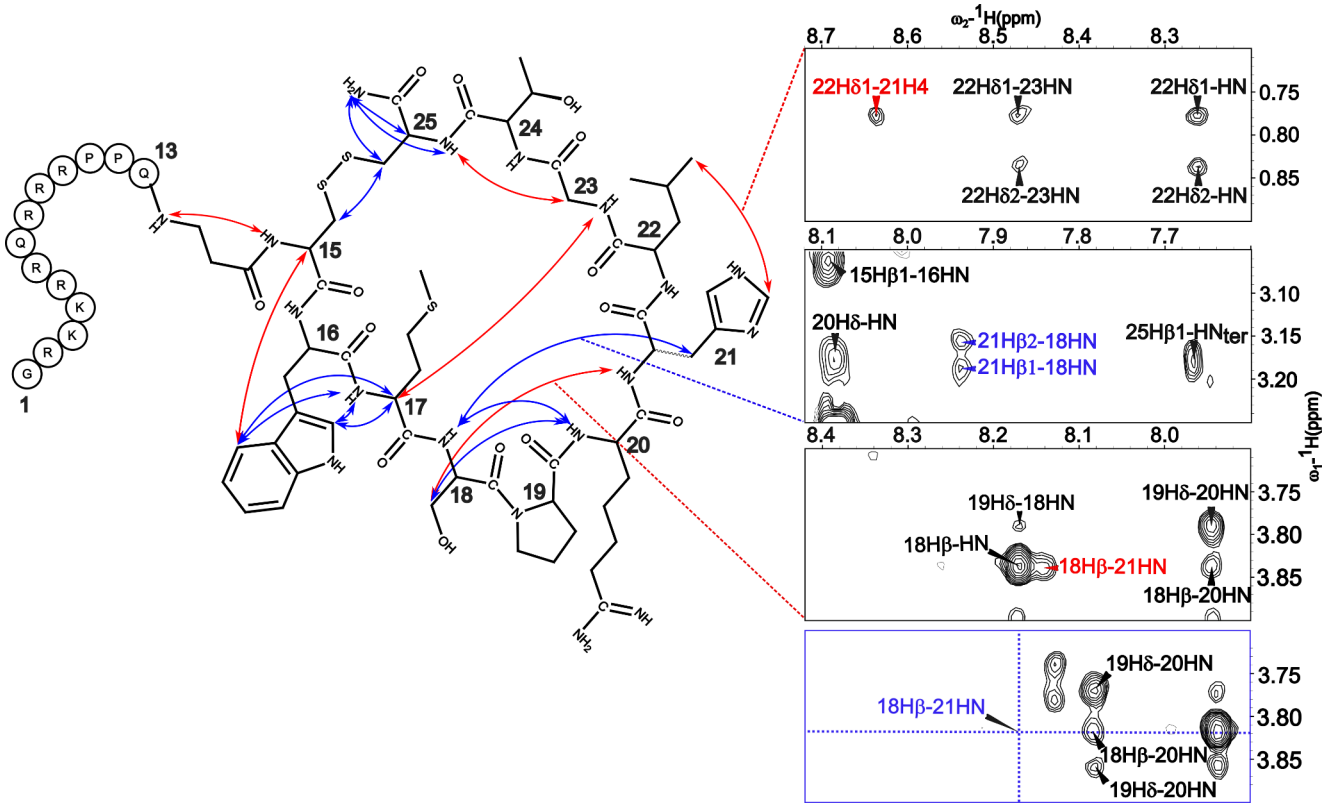

Fig. 2 Characteristics NOE contacts that are only present either in CIGB-300 (blue) or CIGB-300iso (red). The corresponding proton positions are indicated in the structural representation by blue and red arrows for the cyclic part of the CIGB-300 isomers. In the blue box, the absent peak 18Hβ-21H^N for CIGB300 is indicated by dotted lines at the corresponding chemical shift

coefficient also supports the hydrogen bond formation (Fig. S8).

The high-resolution NMR structures of CIGB-300 allowed a classification of the turn conformations. Multiple and continuous turn motives have been described before, and 58% of β-turns occur as multiple turns (Hutchinson and Thornton 1994; Guruprasad et al. 2000, 2001). Even if double turns are the most common, there are reports of triple and higher-order multiple turns (Hutchinson and Thornton 1994). β-turns can be grouped into types I, II, I′, II′, VIa1, VIa2, VIba, and VIII based on the backbone dihedral angles of residue i + 1 and i + 2 (Figure S6). β-turns that do not fit in any of those groups are classified as type IV (Venkatachalam 1968; Richardson 1981; Hutchinson and Thornton 1996). 1/3 of the β-turns in protein correspond to type IV, subdivided into types IV, IV$_1$, IV$_2$, IV$_3$, and IV$_4$ (de Brevern 2016).

The Φ and Ψ dihedral backbone angles of the first and third turn of CIGB-300 do not match with any of the classical groups (Fig. S6), so they were assigned to the miscellaneous category type IV (Fig. S5A and Fig. S5B). The analysis of P19 and R20 dihedral angles allows the classification of a β-turn type IV$_3$ (Fig. 4) (de Brevern 2016). It should be noted that it has been reported that proline in position i + 1 and a trans conformation generally is involved in β-turns of type I and II (Weißhoff et al. 1995). The β-turn type IV$_3$ is similar to type I in its dihedral angle of residue i + 1 but different in its dihedral angle of residue i + 2. Additionally, type IV$_3$ β-turns found in proteins are not associated with either α-helices or β-sheets (de Brevern 2016), a behavior that we also observed in CIGB-300. Also, notice that amino acid i + 3 from the first loop is shared with amino acid i from the second loop, and the third loop continues without common residues otherwise found in triple ββ(i, i + 3)β turns(Hutchinson and Thornton 1994; Guruprasad et al. 2000, 2001).

The structure of CIGB-300iso shows remarkable differences from CIGB-300. The dihedral angles for W16, M17, and L22 correspond to the β-sheet region of the Ramachandran plot (Fig. S5C), and thus an extended conformation. It gets stabilized by hydrogen bonds between the H^N of S18 and CO of D-H21, H^N of D-H21 and CO of S18, and H^N of G23 and CO of W16 CO (black dotted lines in Fig. 3D). The H^N temperature coefficients for CIGB-300iso were different from that of CIGB300 (Fig. S8) and support the hydrogen bond pattern found from these structural elucidations. Interestingly, the presence of D-H21 reduces the number of β-turns to just one between residues S18 to H21. The

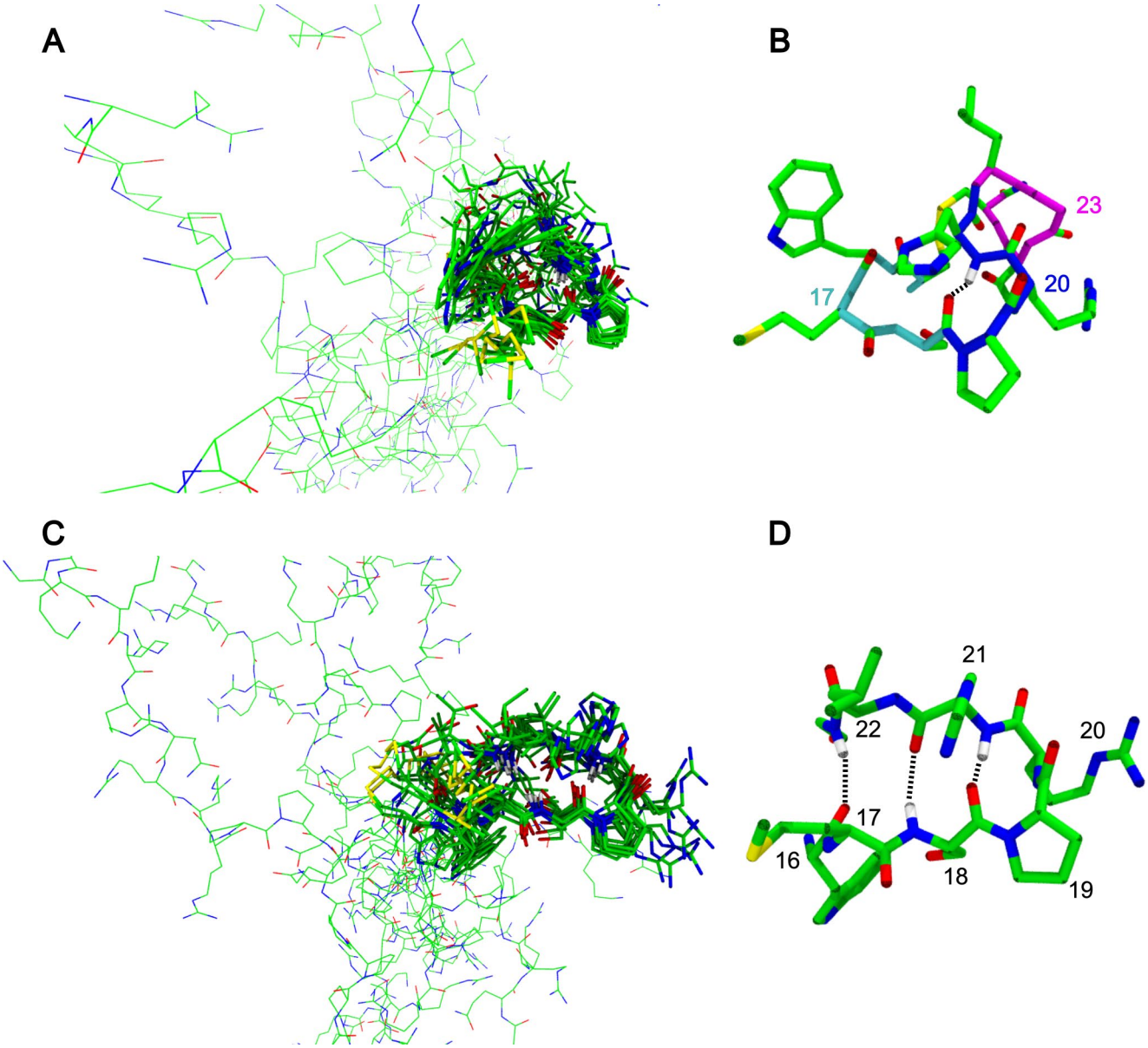

Fig. 3 NMR-derived structures of CIGB-300 and CIGB-300iso. (**A**) Superposition of the 10 NMR structures with the lowest energies of peptide CIGB-300. The TAT region from G1 to βA14 is depicted with narrow lines and the cyclic part from C15 to C25 in a licorice representation. (**B**) The backbone of the different β-turns present in the structure of CIGB-300 are highlighted, the first β-turn from C15 to S18 in light blue, the second β-turn from S18 to H21 in dark blue, and the third β-turn from L22 to C25 in magenta. (**C**) Corresponding superposition of the 10 lowest energy NMR structures of peptide CIGB-300iso. (**D**) Representation of the small β−hairpin in the CIGB300iso. Black dotted lines in (**B**) and (**D**) represent hydrogen bonds

hydrogen bound between the carbonyl of S18 and the amide proton of H21 restricts the average distance between the Cα carbons of the mentioned amino acids to 5.02 ± 0.26 Å.

The dihedral angle analysis of amino acids P19 and R20 reveals a β-turn type I instead of the type IV_3 observed in the CIGB-300 (Fig. 4). D-amino acids can promote the stabilization of the β-turns, where all systematic studies found the D-amino acids in positions i + 1 and i + 2 (Imperiali et al. 1992; Weißhoff et al. 1999; Mitchell and Smith 2003), but best to our knowledge we did not find any report for position i + 3. Anyhow, literature reports show D-amino acids in β-turn type I but in position i, and type VI in position i + 3 (Mitchell and Smith 2003). The β-turn type I is not well known to promote β-hairpin in natural proteins, but there are some reports, especially in synthetic peptides (Sibanda and Thornton 1985; Alba et al. 1999). β-turns are generally considered the initiation site for β-sheet formation, and their sequence plays an important role in the stabilization and classification of β-hairpins(Alba et al. 1999).

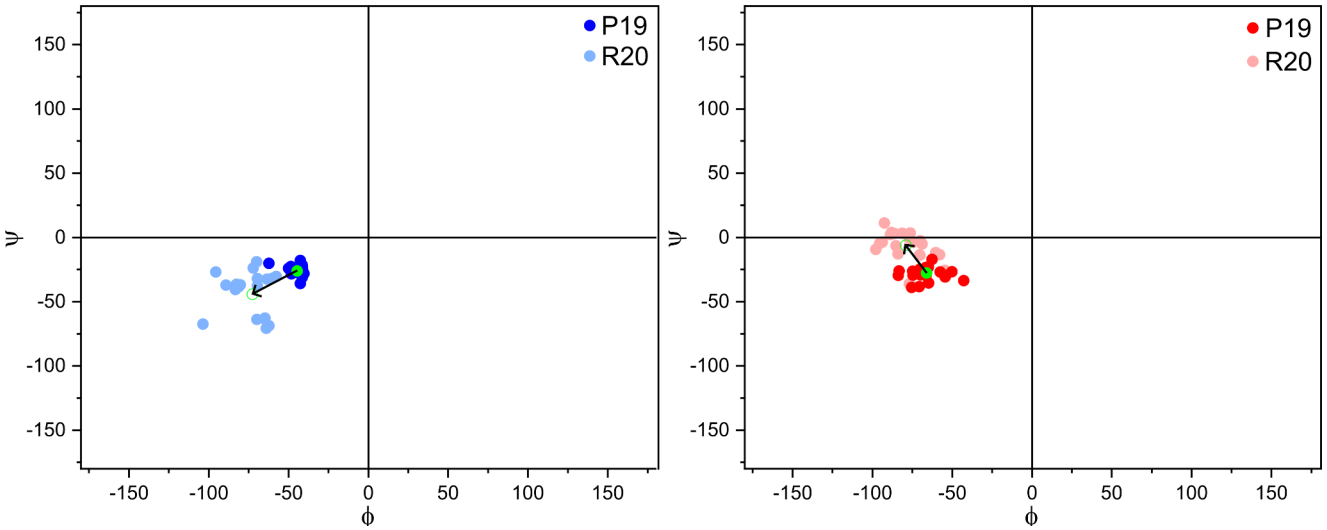

Fig. 4 Ramachandran plots of CIGB-300 (left) and CIGB-300iso (right). The Θ and Ψ values are given for P19 and R20 in the ensemble of twenty lowest energy NMR structures. The green circles represent the average angles for each residue and the shift from residue i + 1 to i + 2 for β-turn classification is represented with an arrow, based on the Thorthon methodology (Hutchinson and Thornton 1994). CIGB-300 (blue, left) represents a distribution characteristic of β-turn type IV_3, and the CIGB-300iso (red) a characteristic of β-turn type I

As we have discussed, the D- or L-form of H21 determines the super secondary structure of the CIGB-300 peptide. The main difference at the i + 3 turn position is not only a classification matter; the change in the super secondary structure leads to different orientations of the local side chains and, therefore, probably differences in the activation of the molecular targets. In a previous alanine scanning, W16 and L22 were identified as important amino acids for anticancer activity (data not shown). The two CIGB-300 diastereomers show various sidechain orientations. In CIGB-300 residue, W16, M17, and H21 face each other, the S18 is oriented to the center of loop one, and the side chains of L22 and T24 are more isolated and exposed. On the other hand, in CIGB-300iso, the side chains of M17, D-H21, and L22 are on the same side of the cyclic peptide part, whereas for W16, S18, and T24, the side chains are oriented towards the opposite side. R20 shows a very similar orientation in both peptides. Notably, the deprotonation of histidine due to pH change in both peptides observed in their NMR spectra promote very small changes in the side chains according to the calculated variance of the aliphatic region in the 1D ^{1}H NMR spectra recorded at pH 3 and 7 ($s^2 = 0.0152$ for CIGB-300 and $s^2 = 0.0243$ for CIGB-300iso). This indicates that the presented structure determined at low pH is very similar to the structure at a more physiological pH.

Conclusion

This study successfully identified a diastereomer formed during the synthesis of the CIGB-300 peptide containing His21 as the sole D amino acid. The change of this L- to D-histidine in the peptide sequence transforms the β-turn type IV_3 present in the CIGB-300 into type I in CIGB-300iso. In consequence, the super secondary structure of both peptides is considerably different, while CIGB-300 adopts a multi-loop structure and the CIGB-300iso forms a small β-hairpin. Both forms also differ considerably in their side chain orientations from which we expect a different biological activity. Therefore, the CIGB-300 diastereomers need to be separated after synthesis during quality control of the anti-cancer peptides and treated separately during cell biological activity tests and subsequent clinical trails.

Supplementary Information The online version contains supplementary material available at https://doi.org/10.1007/s10989-024-10662-2.

Acknowledgements We thank DAAD for funding 'Research Grants - Bi-nationally Supervised Doctoral Degrees/Cotutelle, 2020/21' (program number 57507869) and the German research foundation (DFG grand BA1821/7-1 within the research unit 5433). We also acknowledge significant investments in our NMR facility by the European Regional Development Fund (ERDF) of the European Union. We are further thankful to Dr. Luis J. Gonzalez for all the coordination with the Centre for Genetic Engineering and Biotechnology.

Author Contributions Celia G. Moya, Carlos S. Perez, Hilda Garay, and Jochen Balbach. contributed to the design of the experiments. Material preparation and data collection involved Celia G. Moya, Stefan Gröger, Hilda Garay, and Yordanka Masforrol. The analysis was performed by Celia G. Moya, Rafael Rodriguez, Julian Wiesent, Carlos S. Perez., Jochen Balbach, Yasser Perera, and Silvio E. Perea. The first draft of the manuscript was written by Celia G. Moya. and Rafael Rodriguez, Jochen Balbach, and Carlos S. Perez edited and corrected the final version and all authors commented on the manuscript. Celia G. Moya prepared all the figures and tables, and Rafael Rodriguez contributed to the preparation of Figs. 1 and 4. All authors read and approved the final manuscript.

Funding Celia G. Moya was supported by the DAAD funding 'Research Grants - Bi-nationally Supervised Doctoral Degrees/Cotutelle, 2020/21', funding program number 57507869. Stefan Gröger and Jochen Balbach were funded by the German research foundation (DFG grand BA1821/7 − 1 within the research unit 5433: RNA in focus (RIF)) and Celia G. Moya and Jochen Balbach by the Collaborative Research Centre 1664 'Plant Proteoform Diversity – SNP2Prot' within project B04, funded by the German research foundation (DFG - 514901783). The employed NMR facility was supported by the European Regional Development Fund (ERDF) of the European Union. The Authors have no conflicts of interest to declare that are relevant to the content of this article.
Open Access funding enabled and organized by Projekt DEAL.

Data Availability Original data are available on request from the corresponding author.

Declarations

Competing Interests The authors declare no competing interests.

References

Ahmed K, Issinger O-G, Szyszka R (eds) (2015) Protein kinase CK2 Cellular function in normal and Disease States. Springer International Publishing, Cham

Alba ED, Rico M, Jiménez MA (1999) The turn sequence directs β-strand alignment in designed β-hairpins. Protein Sci 8:2234–2244. https://doi.org/10.1110/ps.8.11.2234

Behrendt R, White P, Offer J (2016) Advances in Fmoc solid-phase peptide synthesis. J Pept Sci 22:4–27. https://doi.org/10.1002/psc.2836

Chiari M, Chiesa C, Righetti PG et al (1990) Kinetics of cysteine oxidation in immobilized pH gradient gels. J Chromatogr A 499:699–711. https://doi.org/10.1016/S0021-9673(00)97014-6

Chou KC (2000) Prediction of tight turns and their types in proteins. Anal Biochem 286:1–16. https://doi.org/10.1006/abio.2000.4757

Cierpicki T, Otlewski J (2001) Amide Proton temperature coefficients as hydrogen bond indicators in proteins. J Biomol NMR 21:249–261. https://doi.org/10.1023/a:1012911329730

de Brevern AG (2016) Extension of the classical classification of β-turns. Sci Rep 6:33191. https://doi.org/10.1038/srep33191

Fields GB, Noble RL (1990) Solid phase peptide synthesis utilizing 9-fluorenylmethoxycarbonyl amino acids. Int J Pept Protein Res 35:161–214. https://doi.org/10.1111/j.1399-3011.1990.tb00939.x

Garay H, Espinosa LA, Perera Y et al (2018) Characterization of low-abundance species in the active pharmaceutical ingredient of CIGB-300: a clinical-grade anticancer synthetic peptide. J Pept Sci 24:e3081. https://doi.org/10.1002/psc.3081

Guruprasad K, Prasad MS, Kumar GR (2000) Analysis of γβ, βγ, γγ, ββ multiple turns in proteins. J Pept Res 56:250–263. https://doi.org/10.1034/j.1399-3011.2000.00739.x

Guruprasad K, Prasad MS, Kumar GR (2001) Analysis of gammabeta, betagamma, gammagamma, betabeta continuous turns in proteins. J Pept Res off J Am Pept Soc 57:292–300. https://doi.org/10.1046/j.1397-002x.2000.00822.x

Han Y, Albericio F, Barany G (1997) Occurrence and minimization of Cysteine racemization during stepwise solid-phase peptide Synthesis1,2. J Org Chem 62:4307–4312. https://doi.org/10.1021/jo9622744

Helmus JJ, Jaroniec CP (2013) Nmrglue: an open source Python package for the analysis of multidimensional NMR data. J Biomol NMR 55:355–367. https://doi.org/10.1007/s10858-013-9718-x

Hutchinson EG, Thornton JM (1994) A revised set of potentials for beta-turn formation in proteins. Protein Sci Publ Protein Soc 3:2207–2216

Hutchinson EG, Thornton JM (1996) PROMOTIF—A program to identify and analyze structural motifs in proteins. Protein Sci 5:212–220. https://doi.org/10.1002/pro.5560050204

Imperiali B, Moats RA, Fisher SL, Prins TJ (1992) A conformational study of peptides with the general structure Ac-L-Xaa-Pro-D-Xaa-L-Xaa-NH2: spectroscopic evidence for a peptide with significant.beta.-turn character in water and in dimethyl sulfoxide. J Am Chem Soc 114:3182–3188. https://doi.org/10.1021/ja00035a002

Kaiser E, Colescott RL, Bossinger CD, Cook PI (1970) Color test for detection of free terminal amino groups in the solid-phase synthesis of peptides. Anal Biochem 34:595–598. https://doi.org/10.1016/0003-2697(70)90146-6

Kovacs J, Kim S, Holleran E, Gorycki P (1985) Studies on the racemization and coupling of N.alpha.,Nim-protected histidine active esters. J Org Chem 50:1497–1504. https://doi.org/10.1021/jo00209a027

Lee W, Tonelli M, Markley JL (2015) NMRFAM-SPARKY: enhanced software for biomolecular NMR spectroscopy. Bioinformatics 31:1325–1327. https://doi.org/10.1093/bioinformatics/btu830

Lewis PN, Momany FA, Scheraga HA (1973) Chain reversals in proteins. Biochim Biophys Acta BBA - Protein Struct 303:211–229. https://doi.org/10.1016/0005-2795(73)90350-4

Mitchell JBO, Smith J (2003) D-amino acid residues in peptides and proteins. Proteins Struct Funct Bioinforma 50:563–571. https://doi.org/10.1002/prot.10320

Morash B, Sarker M, Rainey JK (2018) Concentration-dependent changes to diffusion and chemical shift of internal standard molecules in aqueous and micellar solutions. J Biomol NMR 71:79–89. https://doi.org/10.1007/s10858-018-0194-1

Niefind K, Guerra B, Ermakowa I, Issinger O (2001) Crystal structure of human protein kinase CK2: insights into basic properties of the CK2 holoenzyme. EMBO J 20:5320–5331. https://doi.org/10.1093/emboj/20.19.5320

Pennington MW, Dunn BM (1994) Peptide synthesis protocols. Humana, Totowa, N.J.

Perera Y, Costales HC, Diaz Y et al (2012) Sensitivity of tumor cells towards CIGB-300 anticancer peptide relies on its nucleolar localization. J Pept Sci 18:215–223. https://doi.org/10.1002/psc.1432

Perera Y, Ramos Y, Padrón G et al (2020) CIGB-300 anticancer peptide regulates the protein kinase CK2-dependent phosphoproteome. Mol Cell Biochem 470:63–75. https://doi.org/10.1007/s11010-020-03747-1

Pérez GV, Rosales M, Ramón AC et al (2023) CIGB-300 anticancer peptide differentially interacts with CK2 subunits and regulates specific signaling mediators in a highly sensitive large cell lung Carcinoma Cell Model. Biomedicines 11:43. https://doi.org/10.3390/biomedicines11010043

Piotto M, Saudek V, Sklenář V (1992) Gradient-tailored excitation for single-quantum NMR spectroscopy of aqueous solutions. J Biomol NMR 2:661–665. https://doi.org/10.1007/BF02192855

Richardson JS (1981) The anatomy and taxonomy of protein structure. Adv Protein Chem 34:167–339. https://doi.org/10.1016/s0065-3233(08)60520-3

Roffey SE, Litchfield DW (2021) CK2 regulation: perspectives in 2021. Biomedicines 9:1361. https://doi.org/10.3390/biomedicines9101361

Schwieters CD, Kuszewski JJ, Tjandra N, Marius Clore G (2003) The Xplor-NIH NMR molecular structure determination package. J Magn Reson 160:65–73. https://doi.org/10.1016/S1090-7807(02)00014-9

Schwieters CD, Kuszewski JJ, Marius Clore G (2006) Using Xplor–NIH for NMR molecular structure determination. Prog Nucl Magn Reson Spectrosc 48:47–62. https://doi.org/10.1016/j.pnmrs.2005.10.001

Schwieters CD, Bermejo GA, Clore GM (2018) Xplor-NIH for molecular structure determination from NMR and other data sources. Protein Sci 27:26–40. https://doi.org/10.1002/pro.3248

Shen Y, Bax A (2015) Protein structural information derived from NMR Chemical Shift with the neural network program TALOS-N. In: Cartwright H (ed) Artificial neural networks. Springer, New York, NY, pp 17–32

Shen Y, Delaglio F, Cornilescu G, Bax A (2009) TALOS+: a hybrid method for predicting protein backbone torsion angles from NMR chemical shifts. J Biomol NMR 44:213–223. https://doi.org/10.1007/s10858-009-9333-z

Sibanda BL, Thornton JM (1985) β-Hairpin families in globular proteins. Nature 316:170–174. https://doi.org/10.1038/316170a0

Subirós-Funosas R, Prohens R, Barbas R et al (2009) Oxyma: an efficient additive for peptide synthesis to replace the benzotriazole-based HOBt and HOAt with a lower risk of explosion. Chem Weinh Bergstr Ger 15:9394–9403. https://doi.org/10.1002/chem.200900614

Trembley JH, Wang G, Unger G et al (2009) Protein kinase CK2 in Health and Disease: CK2: a key player in cancer biology. Cell Mol Life Sci 66:1858–1867. https://doi.org/10.1007/s00018-009-9154-y

Venkatachalam CM (1968) Stereochemical criteria for polypeptides and proteins. V. conformation of a system of three linked peptide units. Biopolymers 6:1425–1436. https://doi.org/10.1002/bip.1968.360061006

Weißhoff H, Frost K, Brandt W et al (1995) Novel disulfide-constrained pentapeptides as models for β-VIa turns in proteins. FEBS Lett 372:203–209. https://doi.org/10.1016/0014-5793(95)00982-F

Weißhoff H, Präsang C, Henklein P et al (1999) Mimicry of βII′-turns of proteins in cyclic pentapeptides with one and without d-amino acids. Eur J Biochem 259:776–789. https://doi.org/10.1046/j.1432-1327.1999.00097.x

Wüthrich K (1990) Protein structure determination in solution by NMR spectroscopy. J Biol Chem 265:22059–22062. https://doi.org/10.1016/S0021-9258(18)45665-7

Yang Y, Hansen L, Baldi A (2022) Suppression of simultaneous Fmoc-His(Trt)-OH Racemization and Nα-DIC-Endcapping in solid-phase peptide synthesis through design of experiments and its implication for an amino acid activation strategy in peptide synthesis. Org Process Res Dev 26:2464–2474. https://doi.org/10.1021/acs.oprd.2c00144